

Highlighting Features of Spatiotemporal Spread of Powdery Mildew Epidemics in the Vineyard Using Statistical Modeling on Field Experimental Data

A. Calonnec, P. Cartolaro, and J. Chadœuf

First and second authors: UMR Santé Végétale INRA-ENITA, 71 Avenue Edouard Bourlaux, 33883 Villenave d'Ornon cedex, France; and third author: Station de Biométrie, INRA Domaine St Paul, Site Agroparc, 84914 Avignon cedex 9, France.

Accepted for publication 27 November 2008.

ABSTRACT

Calonnec, A., Cartolaro, P., and Chadœuf, J. 2009. Highlighting features of spatiotemporal spread of powdery mildew epidemics in the vineyard using statistical modeling on field experimental data. *Phytopathology* 99:411–422.

A greater understanding of the development of powdery mildew epidemics on vines would improve disease management by making assessments of the risk of invasion more accurate. We characterized the spatiotemporal spread of epidemics in the vineyard, quantified their variability, and identified the factors responsible for it. We described changes in the probability of infection of a leaf in a plot over time and as a function of distance from a source of disease. Logistic models were fitted to field data from artificially inoculated plots. The velocity of spread decreased along the row and increased in the direction of the prevailing winds. The

rate of progression over time was plot dependent, and the velocity was dependent on the vigor of the vine (0.1 to 0.27 m day⁻¹ in areas of moderate vigor and 1.1 m day⁻¹ in areas of high vigor). When applied to a larger plot with natural primary foci, the spatiotemporal logistic model showed that the velocity and the slope of the gradient in space depended on the foci; however, the velocity remained in the same range. During the period of highest susceptibility for grape, the probability of a leaf becoming infected increased from 2.5 to 13%. Our logistic model was able to predict changes in disease over time of its extension within the plot; however, the crop heterogeneity prevented prediction of variability of disease at the vine scale.

Additional keywords: *Erysiphe necator*, maximum likelihood, parametric bootstrap, *Vitis vinifera*.

Models can be useful for predicting average development and variation of disease. For example, temporal disease progress curves are used for the characterization and comparison of epidemics. The study of the variation in fitted parameters allows the identification of factors favoring disease progression (8,45). However, empirical models must fit the data closely for an accurate comparison of epidemics and elucidation of the mechanisms involved. Spatial components of plant disease epidemics are characterized with mathematical approaches based on dispersal (e.g., use of the observed disease gradient to elucidate the form of contact distribution) or with more statistical approaches involving spatial characterization based on indices (23,31). Statistical approaches of this type may be more directly useful for the development of sampling plans (32) and for guiding decisions concerning control interventions. Several approaches have been developed to estimate epidemiological parameters from spatial disease data (44,46) which differ by the spatial scale or by the number of cycles at which the disease is observed. It is generally most informative to consider both spatial and temporal dynamics when trying to understand and quantify the processes and factors governing the spread of an epidemic and underlying its variability (22,24,25,29,34,42,46). Stochastic models and parameter estimation have been used to consider disease progression and spatial characterization together in situations of moderate spatial heterogeneity, in which the plants are spatially referenced and disease intensity is measured as a binary variable (21,30). Spatiotemporal approaches seem to be particularly useful for studies of disease initiated by isolated foci and spreading on plants in rows, within a

constrained spatial structure (35) changing considerably over time and space, thereby altering the conditions for spore dispersal and the rate of invasion.

Powdery mildew caused by *Erysiphe necator* is the most widespread disease on *Vitis vinifera* worldwide and is the main target for fungicide treatments on grapevines (1,36). The vine is characterized by a high degree of spatial structure at the plant and field levels, exhibiting rapid changes over time. The disease remains difficult to control because (i) there is no forecast system for epidemics initiated by ascospores able to predict the timing and amount of primary infections and (ii) the signs of the disease are difficult to detect in the vineyard in the first 30 to 40 days after the onset of the epidemic (three to four pathogen generations) without careful check. However, the harvest damage to grape berries depends on the early development of the disease on leaves of susceptible cultivars. The leaves are infected first, and there is a spatial relationship between frequency maps for diseased leaves early in the season and frequency maps for bunches of grape with high disease severity later in the season (6,38). Indeed, grape berries are susceptible to the disease over a relatively short period (17–19) and the severity of damage to the grape and the wine (7,11) depends on the number of spores infecting the plant. Blaise and Gessler (4,43) and Sall (4,43) showed that the apparent rate of infection depends on temperature and moisture conditions and that host growth may slow down or even stop infections. These findings were obtained using deterministic models based on modified Van der Plank equations, taking host growth into account. However, these models could not be used to study the dependence of infection rate on spore dispersion or host–pathogen interactions, variations which are nonnegligible at the start of the epidemic. Based on these findings and on our experience, we think that early disease development must be taken into account in efforts to control powdery mildew epidemics. This

Corresponding author: A. Calonnec; E-mail address: calonnec@bordeaux.inra.fr

doi:10.1094/PHYTO-99-4-0411

© 2009 The American Phytopathological Society

may be particularly true for precision agriculture approaches, in which it is necessary to predict the average disease development and changes in disease over space and time.

In this study, powdery mildew epidemics on grapevines were modeled with the aim to (i) characterize disease spread, focusing on disease velocity and disease gradient; (ii) identify factors responsible for variations in disease spread; and (iii) predict spatial variations in disease spread and intensity, based on early disease detection. Deterministic models handled by statistical methods in discrete time are used. With this approach, disease progression can be described with simple models based on small numbers of parameters, and variability can be assessed by analyzing the parameters. We first used a nonspatial logistic model to analyze disease development over time, on plots and for epidemics initiated by a single focus. The limits of this model for prediction are identified. We then used a spatiotemporal logistic model to analyze the variation in disease intensity over time and distance from the source of the initial inoculum. This model may be considered to be a stochastic version of the deterministic model proposed by Jeger (29). The model is first developed at the focus level, on artificially inoculated plots in which the primary infection could be controlled in time and space. The aim was to assess the variability of focus development on different scales (site, plot, and direction) and to identify the scale at which the model was able to identify potential variability factors and to predict spatial variations in disease. We then validated, at plot level, the ability of the model to characterize an epidemic for which several primary natural foci are detected during a first round of inspection, and to predict disease variation.

MATERIALS AND METHODS

Spread of the epidemic from a single focus. *Field experimental design.* The experiment was conducted in 1998 on *V. vinifera* cv. Cabernet-Sauvignon vines in Martillac, Bordeaux (France). The experimental area consisted of three replicate plots (P1, P2, and P3), each containing 49 vines in a vineyard of 85 vines by 23 rows. Spacing was 1 m between vines and 1.5 m between rows. The vines were "guyot" pruned, traditionally topped and trimmed, and sprayed against downy mildew, *Botrytis* spp., and insects when necessary.

Inoculation. Inoculation was performed on 5 May (phenological stage E to F on the Baggioolini scale) (2), as described by Cartolaro and Steva (9), on one shoot of the chosen vine, close to the center of the vine. The inoculated vine was located in the center of the experimental plot. The inoculum consisted of a monoconidial isolate collected from one field the previous year. The vines were almost free from powdery mildew and cleistothecia the year before the experiment. Therefore, the amount of primary inoculum already present in the field was negligible, making it unlikely that primary foci other than those created by inoculation would become established.

Disease assessment. On each of the 49 vines in each plot, the lower surfaces of the leaves of three to four shoots per vine were checked for powdery mildew colonies. Because the precise assessment of disease severity (proportion of leaf area diseased) is time consuming for large samples, we rated disease incidence (proportion of leaves with at least one colony). Shoots were distributed on each of the two main canes and marked at bud break. The number of diseased leaves was assessed during vine growth, from the beginning of June to the end of July, at 31 (4 June), 37 (10 June, beginning of flowering), 45 (18 June), 51 (24 June), 59 (3 July), 65 (9 July), 73 (17 July), 80 (24 July), and 87 (31 July) days after inoculation. Only the vines located on the transects corresponding to the eight cardinal directions were used in the spatial analyses (four vines per transect). Because of the difficulty of detecting powdery mildew colonies early in infection, the same leaves were assessed throughout the entire season,

to confirm the assessments made on previous scoring dates. For each vine, vigor was assessed at the end of July on a scale with five classes corresponding to a visible decrease in leaf density due to the production of smaller numbers of secondary leaves.

Models. Disease development over time was analyzed at plot scale by fitting a logistic model similar to that proposed by Van der Plank (50) to the data, with disease incidence ratings (y) increasing with time (t) as described by equation 1:

$$y = \frac{1}{1 + \exp(K) \exp(-rt)} \quad (1)$$

where y represents the frequency of diseased leaves on the plot at time t , with $K = \ln((1 - y_0)/y_0)$, a parameter related to the quantity of primary inoculum y_0 , and r is a constant indicating the rate of increase of disease per unit per time. There are several assumptions underlying this model: random dispersion (no aggregation), and constant host surface (no host growth) (53).

The progression and spread of disease within plots was studied with a model similar to that proposed by Jeger (29) for polycyclic epidemics with rates of progression independent of time and space. Disease incidence ratings (y) at time (t) and relative to the distance from the source of inoculum (d) can then be described by equation 2:

$$y = \frac{1}{1 + \exp(K) \exp(bd - bct)} \quad (2)$$

where y represents the frequency of diseased leaves in a vine at time t and at a distance d from a primary source of inoculum, assuming that the total number of available leaves is constant over time; b is the rate of decrease in disease with distance from the source (disease gradient slope); and c is the rate of isopath movement (horizontal disease velocity or increase in the disease incidence ratings at distance d and time t) and K has the same signification as for equation 1. At the leaf level,

$$p(d, t) = \frac{1}{1 + \exp(K) \exp(bd - bct)}$$

represents the probability that a leaf at distance d , taken at random at date t , is found to be diseased. Consequently,

$$p(d, t_{k-1}, t_k) = p(d, t_k) - p(d, t_{k-1})$$

is the probability that a leaf at distance d , found to be healthy at date t_{k-1} will be found to be diseased at date t_k . Taking into account the number of diseased and available healthy leaves at each date, the change in this probability corresponds to the change in probability of a leaf becoming infected, as a function of space and time and taking shoot growth into account. Similarly, for the temporal model (equation 1),

$$p(t_{k-1}, t_k) = p(t_k) - p(t_{k-1})$$

is the probability that a leaf, randomly selected from the plot and healthy at date t_{k-1} will be found to be diseased at date t_k . By using a logistic type model, it is assumed that all new colonies on the inoculated plots resulted from disease spread from the inoculated vine.

Spread of the epidemic from multiple natural foci. *Experimental design.* The experimental plot consisted of 330 vines at the INRA experimental station at Couhins in 1999. This plot (P4) had not been treated for powdery mildew during the year before the experiment. P4 consisted of five rows, each containing 66 vines of Cabernet-Sauvignon, with 2 m between rows and 1 m between plants along the row. Pruning was restricted to ensure that there was an average of six shoots per vine. Leaves from two shoots per plant were scored. At the first assessment date (12 May), four foci were located: F1 on row 2 vine 4 (R2-V4), F2 on R2-V19, and F3 and F4 on rows 2 and 3 on vines 35 (R2-V35 and R3-V35). F2

corresponded to a sporulating flag shoot (identified by polymerase chain reaction [PCR] as biotype I or A, as defined earlier) (12,13) whereas F1, F3, and F4 were restricted to small colonies resulting from ascospore infections (biotype III or B). Six assessments were performed, on 12 May, 26 May, 2 June (day 153, beginning of flowering), 15 June, and 1 and 20 July. The natural contamination giving rise to the three foci resulting from ascospore infections was estimated to have occurred on 3 May based on the pattern of rainfall, the phenology of the plot, and the latent period (20,41). Disease assessments were synchronized with the life cycle of the fungus based on the estimated latency period, except at the end of the epidemic (between 1 and 20 July), where approximately two cycles can be expected.

Model. The model used to describe disease spread from multiple foci was derived from equation 2 by introducing an additional parameter (a) to take into account the potential anisotropy of the horizontal disease spread. We defined the distance D_i between an unspecified leaf attached to a vine located at $C(x,y)$ and a vine with primary disease (primary focus) located at $C_i(0,0)$ as follows:

$$D_i = d(C, C_i) = \sqrt{(d_x^2 + a d_y^2)}$$

with d_x being the distance between C and C_i within the row and d_y the distance between C and C_i across rows.

Assuming that each leaf on an unspecified vine V could be contaminated independently by spores from each of the I primary foci between dates t_{k-1} and t_k , the probability $(1 - P)$ for that leaf to be diseased verifies the relationship:

$$1 - P(V, t_{k-1}, t_k) = \prod_{i=1, \dots, I} [1 - p(D_i, t_{k-1}, t_k)]$$

where $p(D_i, t_{k-1}, t_k)$ is the probability of each leaf, located at position C , at a distance D_i from a focus located at position C_i becoming contaminated between dates t_{k-1} and t_k , with

$$p(D_i, t_{k-1}, t_k) = \frac{1}{1 + \exp(K) \exp(b D_i - b c t_k)} - \frac{1}{1 + \exp(K) \exp(b D_i - b c t_{k-1})}$$

Using the logistic model, we assumed that all new colonies observed in the plot resulted from dispersion from the four primary foci.

Statistics. The general approach was to (i) assess the values of the parameters by maximum likelihood methods; (ii) determine, using likelihood-ratio tests, the pertinent scale for parameter assessment to rule out several hypotheses about the spread of the epidemic, (iii) determine confidence intervals for each of the parameters allowing the identification, through comparisons, of factors altering the velocity with which the epidemic spreads; and (iv) validate the model by comparing different variables of interest calculated from the data with those obtained from simulations, based on the parameter values provided by the estimation procedure. The variables studied were (i) changes in the frequency of newly diseased leaves over time, (ii) a variogram to measure the intraplot variability, and (iii) changes over time in the average number of newly infected leaves in a row to measure disease spread.

Parameter estimation. Parameters were estimated using maximum likelihood methods (10). $N_{d_v,k}$ is the number of healthy leaves at date k on a vine v at distance d from the source and $n_{d_v,k-1,k}$ is the number of leaves infected between dates $k-1$ and k on this vine. Assuming that the leaves are independent, the probability of these leaves $n_{d_v,k-1,k}$ becoming infected, among the total number of leaves available for infection ($N_{d_v,k} + n_{d_v,k-1,k}$) follows the binomial probability distribution:

$$P = \prod_{v=1}^V \prod_{k=2}^K C_{n_{d_v,k-1,k}}^{N_{d_v,k} + n_{d_v,k-1,k}} [p(d_v, t_{k-1}, t_k)]^{n_{d_v,k-1,k}} (1 - p(d_v, t_{k-1}, t_k))^{N_{d_v,k}}$$

with V and K corresponding to the total number of vines and evaluation dates, respectively.

Parameters were estimated such that P was maximal or the L was minimal, with

$$L = -\ln(P) = \sum \ln \left(C_{n_{d_v,k-1,k}}^{N_{d_v,k} + n_{d_v,k-1,k}} \right) + \sum_{k=2}^K \left\{ \sum_{v=1}^V n_{d_v,k-1,k} \ln(p(d_v, t_{k-1}, t_k)) - \sum_{v=1}^V N_{d_v,k} \ln(1 - p(d_v, t_{k-1}, t_k)) \right\}$$

The likelihood of the spread of the epidemic from multiple natural foci is

$$P = \prod_{V \in V} \prod_{k=2, \dots, K} \left\{ P(V, t_{k-1}, t_k)^{n_{d_v,k-1,k}} [1 - P(V, t_{k-1}, t_k)]^{N_{d_v,k}} \right\}$$

Hypothesis testing. In the experiment in which plots were artificially inoculated, likelihood ratio tests were used to determine the most pertinent level for parameter estimation (overall experiment, plot, direction, or direction per plot). Three submodels were defined: m_1 , identical parameters for the three plots; m_2 , different parameters for the different plots; and m_3 , parameters dependent on the eight cardinal directions. The consistency of these submodels was assessed by comparison with the more complex general model (m_G), including one parameter per cardinal direction for each experimental plot. This made it possible to test the following hypotheses: no effect of plot or direction on spread ($m_1 = m_G$), a plot effect but no direction effect ($m_2 = m_G$), or same direction of spread for the three plots ($m_3 = m_G$) (Table 1). Models were compared using likelihood ratio tests (10). The principle was to restrict the parameters in the likelihood expression, thereby reducing the total number of unknown parameters. Similarly, in the naturally infected plot experiment, likelihood

TABLE 1. Hypothesis testing for a spatiotemporal disease progress model for grape powdery mildew from one single focus

Level studied	Model ^y			Likelihood-ratio test	
	Designation	Estimated parameters ^z	No. of parameters	Models compared	Tested hypothesis
Overall experiment	m1	K b c	3	m1–mG	No plot or direction effect
Experimental plot	m2	K _p b _p c _p	9	m2–mG	Plot effect, no direction effect
Direction	m3	K _D b _D c _D	24	m3–mG	Same direction effect for the three plots
Direction per plot	mG	K _{p,D} b _{p,D} c _{p,D}	72

^y Equation: $p(d,t) = 1/(1 + \exp[K] \exp[b d - b c t])$, where K = a constant related to the quantity of primary inoculum, b = the rate of decrease of the disease severity with the distance to the source, and c = disease velocity.

^z Index P and D indicate dependence on plot (P1, P2, or P3) and cardinal direction, respectively.

ratio tests were used to identify the most pertinent level for each parameter studied (focus or plot) and to test hypotheses about disease spread (Table 2). In the more complex general model (m_G), spread is dependent on time and on each primary focus. Note that the power of the test depends of the number of available data.

Confidence intervals of the parameters. Once a model was chosen, profile likelihood confidence intervals ($\alpha = 5\%$) were calculated for each parameter (51). For a given parameter θ , let $L(\theta) = \log(P(\theta))$ be the profile-likelihood at θ (i.e., the value of the logarithm of likelihood at value θ , with maximization for the other parameters). If $\hat{\theta}$ denotes the estimated parameter, the confidence interval is defined as the set of all θ such that $2(\log(\hat{\theta}) - \log(\theta)) \leq q(\alpha)$, with $q(\alpha)$ the $(1 - \alpha)$ th percentile of the χ^2 distribution with 1 degree of freedom (df). This confidence intervals are based on asymptotic results; the more the data, the more exact are the confidence interval.

Model validation. The variability in statistical models results from their stochastic component (an individual leaf has only a certain probability of being diseased) and from the variability of the estimated parameters. Both types of variability were taken into account, using a parametric bootstrap (14). For the single-focus model, based on the binomial distribution of the estimated probability, we simulated changes in leaf infection 1,000 times for each vine (spatial model) or each plot (temporal model) at each time point, so as to obtain a set of values for newly infected leaves. The confidence interval was obtained by calculating quantiles for this set of values. The observed values of the probability of leaves to be infected were compared with simulated values in two-tailed tests with a significance level of 5%. For the multiple-focus model, three variables of interest providing a description of the disease on various scales were calculated. The first variable studied was the change over time in the frequency of newly diseased leaves at the plot level. The second variable studied was the change over time in the number of newly infected leaves as a function of the distance (d) between vines at the within-plots level (a measure of the within-plots variability). This variable is represented, for each assessment date ($k + 1$), by the variogram:

$$\gamma(d) = \frac{1}{J(I-d)} \sum_j \sum_{i=d}^J (n_i - n_{i+d})^2$$

where I and J are the vine and row numbers, respectively, and n_i and n_{i+d} are the number of newly infected leaves on vines i and $i + d$, respectively. This empirical variogram measured the similarity between plant disease levels depending on their distance. The third variable was the change over time in the average number of newly infected leaves in a given row (a measure of the disease extension along the row)

$$E(i, j) = \frac{1}{i} \sum_{j=1}^j n_i$$

with n_i the number of newly infected leaves on vines i in row j . Observed values of these variables of interest were compared graphically with simulated values.

RESULTS

Spread of the epidemic from a single focus. *Description of the disease: a high level of variation between plots with common characteristics of disease spread.* The temporal progression of the disease on individual plots assessed by measuring the incidence of disease on leaves (mean proportion of leaves per vine with at least one colony) or the incidence of the disease on vines (mean proportion of vines with at least one diseased leaf) followed an S-shaped curve for P2 and P3 (Fig. 1). For P1, the observations of the incidence of disease on leaves stop before they reach an asymptote. The temporal progression of the disease was highly variable on the three plots, with a frequency of diseased leaves at the end of the season of 33% (P1) to 86% (P2). The empirical evolution of the incidence of disease on leaves versus the incidence of disease on vines (Fig. 2) does not show much discrepancy with a distribution of diseased leaves under the assumption of a binomial distribution (infected leaves uniformly distributed

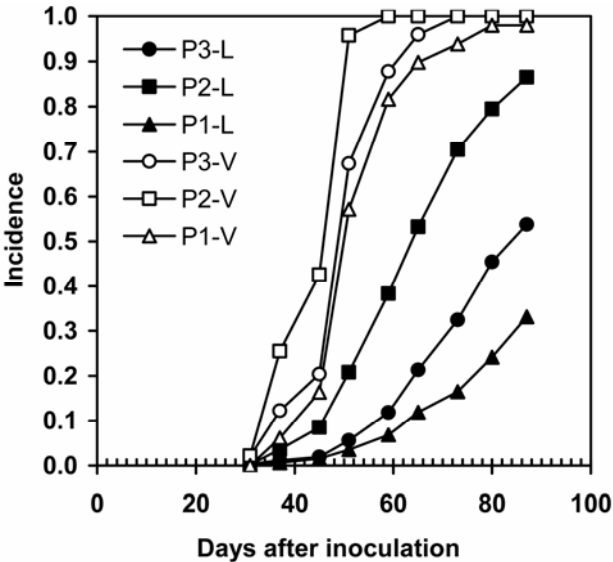


Fig. 1. Progression of powdery mildew over time in three grapevine plots—P1, P2, and P3 (49 vines per plot)—inoculated at the center. The closed symbols indicate the progression of the disease when incidence was assessed at the individual leaf scale (L) (average proportion of leaves per vine with at least one colony) and the open symbols indicate the progression of the disease when incidence was assessed at the vine scale (V) (average proportion of vines with at least one diseased leaf).

TABLE 2. Hypothesis testing for a spatiotemporal disease progress model for grape powdery mildew from multiple foci

Model ^x			Likelihood-ratio test		
Designation	Parameters ^y	Models compared	Tested hypotheses	L value	Result ^z
MG	K _{i,t} b _{i,t} a _{i,t}	...	Spread of the disease dependent on time, parameters different for each primary focus i	12,616.8	...
M1	K _i b _i c _i a _i	M1MG	Spread of the disease independent on time, parameters different for each i	12,638.1	A
M2	K _i b _i c _i a	M2M1	Parameter a identical for each i (same anisotropy), K , b , c focus dependent	12,638.8	A
M3	K b c a	M3M2	a , K , b , c identical for each i	12,884.9	R
M4	K b _i c _i a	M4M2	a and K identical for each i	12,652	R
M5	K _i b c _i a	M5M2	a and b identical for each i	12,664.8	R
M6	K _i b _i c a	M6M2	a and c identical for each i	12,660.6	R

^x For MG, the model is $p(d,t) = 1/(1 + \exp[K] \exp[bd])$ with $d = \sqrt{d_x^2 + ad_y^2}$. For submodels M1 to M6, the model corresponds to equation 3: $p(d,t) = 1/(1 + \exp[K] \exp[bd - bct])$ with $d = \sqrt{d_x^2 + ad_y^2}$, the distance between any vine and the different primary foci.

^y Estimated parameters: K = constant related to the quantity of primary inoculum, the rate of decrease of the disease severity with the distance d to the source, c = disease velocity, and a = anisotropy of the horizontal disease spread. Index i and t = primary focus and time.

^z A and R indicate accepted and rejected, respectively.

among all vines). Only P2 displayed a slightly more aggregated pattern of disease (Fig. 2). However, aggregation levels remained low, with 20% of the leaves diseased and 95% of vines affected at 50 or 65 days (plot P2 or P3, respectively) after inoculation (Figs. 1 and 2). This high level of spread was reached only 76 days after inoculation on plot P1. Spatial heterogeneity was also observed, with a high frequency of diseased leaves along the west and northwest directions of plot P2, and the highest frequency of diseased leaves lying in the direction of the prevailing wind (east and northeast) for plot P3 (Fig. 3). In plot P1, disease severity decreased toward the north. The spatial differences in disease

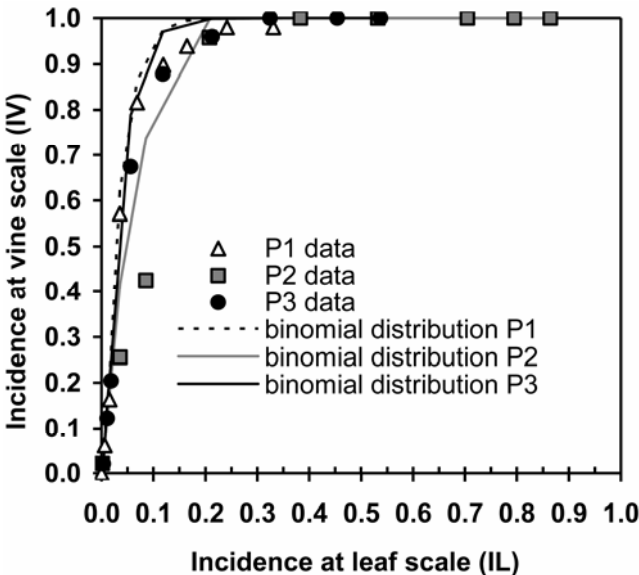


Fig. 2. Observed relationship between two levels of spatial hierarchy of grape powdery mildew: incidence at leaf scale (IL = proportion of diseased leaves per vine with at least one colony) and incidence at vine scale (IV = proportion of vines with at least one diseased leaf) for three plots (P1, P2, and P3), and simulated relationship according to a binomial distribution of infected leaves ($IV = 1 - [1 - IL]^{\text{leaves number}}$) (27,33).

spread between the three plots appeared to be related to the vigor of the vines (Fig. 4).

Disease progression over time: the early part of the epidemic is well described by the logistic model. A leaf becoming infected

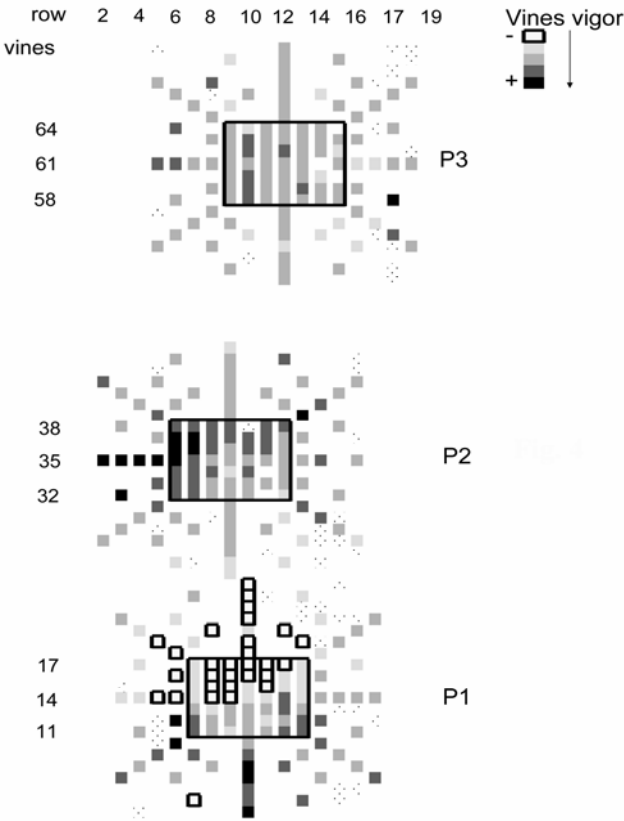


Fig. 4. Assessments for vine vigor on 30 July, based on a visual scale of five classes corresponding to a visible decrease in leaf density. Selected plots (P1, P2, and P3) of 49 vines were studied and the location of each vine is indicated with a vine and row rank on the overall experimental plot.

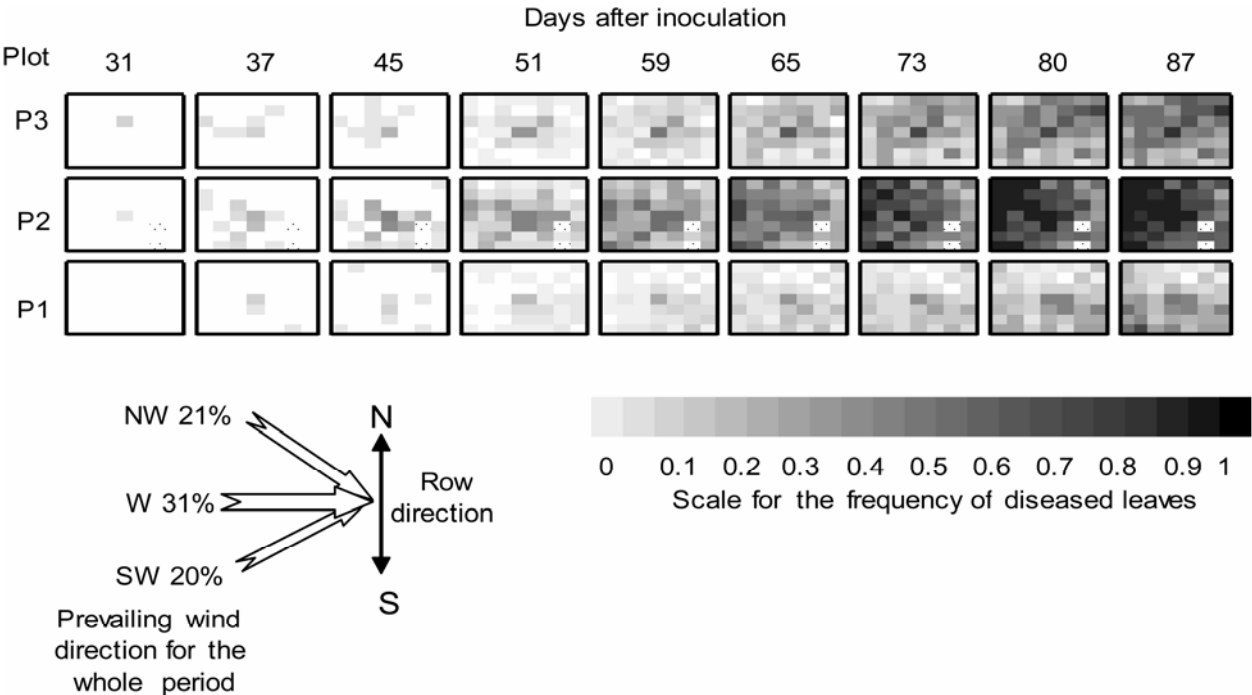


Fig. 3. Epidemic spread of grape powdery mildew in the 49-vine plots P1, P2, and P3, in which the central vine was inoculated on 5 May. The frequency of diseased leaves on each vine (square) is indicated on a gray scale. For the central vine, the inoculated shoot is not included in the calculation of frequency.

was accurately described by the temporal logistic model (equation 1) for plots P3 and P1, provided it was restricted to the first eight assessment dates, and for plot P2, provided it was restricted to the first five dates, and even then, predictions were poor for some dates (Fig. 5). Based on the first part of the epidemic (the first five dates), the rate of infection over time differed significantly between three plots, reaching 0.08 for P1, 0.10 for P3, and 0.13 for P2, with no significant difference in K (7.28 for P1, 7.97 for P3, and 7.85 for P2, with the corresponding likelihood values of 425.9, 619.4, and 1,342), indicating no significant difference in primary inoculation. Between 37 and 51 days after inoculation—a period during which young berries were highly susceptible to infection—the probability of a leaf becoming infected increased from 3 to 10% for P2 and from <1 to 2% for P3. For plot P2, the frequency of diseased leaves was >0.5 beyond 59 days after infection. Due to the symmetry of the logistic model, a decrease of $p(t_{k-1}, t_k)$ was predicted, whereas the observed probability (available healthy leaves becoming diseased) actually continued to increase until day 73. By day 59, the disease had spread to every vine in P2. This may have increased the probability of new leaves becoming diseased on each vine and may, therefore, represent the limit of validity of the logistic model.

Characterization of disease progression in space: a high level of within-plots variation related to the variation in vine vigor. Likelihood ratio tests comparing the spread of the epidemic from a single focus (equation 2), at different levels, showed that a hypothesis predicting a common pattern of behavior at any site or plot or in any particular direction could be rejected (Table 3). Global disease spread was better described by the most complex model (m_G), based on direction per plot. Most of the differences between the submodels and the general model were due to high levels of variation in the slope of disease gradient in space (b), which varied with the plot and the direction: b varied from 0.12 (P2, direction 7 [west]) to 1.99 (P1, direction 1 [north]) (Table 3; Fig. 6). The slope of disease gradient was especially lower (wider spread) in the areas in which plant vigor was greatest (compare directions 6 and 7 with directions 1 and 2 in plot P2) (Table 3).

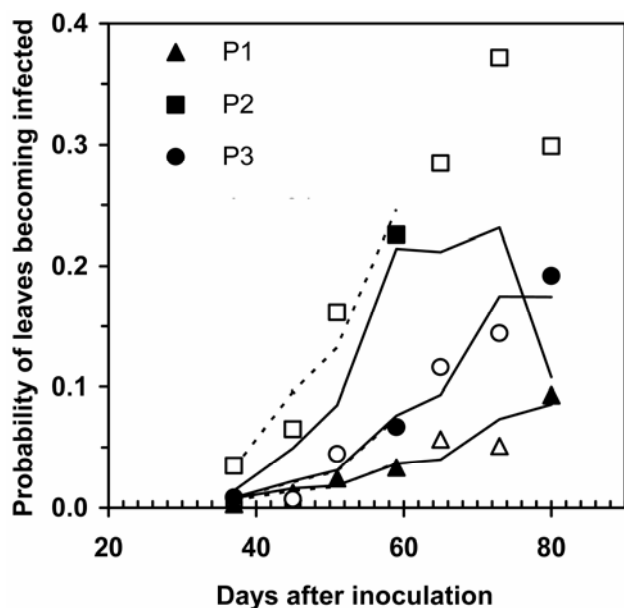


Fig. 5. Estimated (lines) and observed (symbols) probabilities of leaves becoming infected with grape powdery mildew for the three plots (P1, P2, and P3) for the temporal model equation 1. Observed data at day k are the number of newly infected leaves per total number of healthy leaves at $k - 1$ plus the total of leaves emerging between k and $k - 1$. Solid line: assessments based on all eight dates; dashed lines: assessments based on the first five dates. The goodness of fit of each point is indicated by its color (black for $P < 0.025$ or > 0.975 , white for $0.025 < P < 0.975$).

Plot P3, with the most homogeneous levels of vine vigor, had the smallest slope for disease gradient in the direction of the prevailing winds (compare directions 2 to 3 with directions 6 to 7) (Table 3). In contrast, b was steeper, either because of low vigor (direction 1 for P1) or because of row direction (direction 5 for P2 and P3) when compared with the values on either side (directions 4 and 6). Thus, on average, the disease could spread by up to $c = 1.1$ m day⁻¹ in the zones of highest vigor on plot P2 (directions 6 and 7) and spread very little, at $c = 0.04$ m day⁻¹, in the low-vigor zones of P1 (direction 1). These results suggest that the disease may spread twice as fast in the direction of the prevailing wind than in other directions. For example, the velocity of spread on plot P3 reached a mean of 0.26 m day⁻¹ for directions 2 to 3, versus only 0.15 m day⁻¹ for directions 6 to 7. Furthermore, the velocity of spread may be up to six times higher in a zone of high vigor than in a zone of moderate vigor, reaching 1.05 m day⁻¹ in plot P2 for directions 6 to 7. Along the rows (continuous canopy), the mean rate of disease velocity of spread remained at 0.15 m day⁻¹ for the entire epidemic period.

Parameter K , related to primary disease level, was almost isotropic and could be approximated by an equation defining a circle. It differs significantly between the various plots and directions and tended to be lower in zones of low vigor (P1, directions 1, 2, and 8).

Model validation: the early part of the epidemic is well predicted by the spatiotemporal logistic model. Based on the simulated number of infected leaves at each distance and time, the spatiotemporal logistic model (equation 2) correctly predicted disease variations at vine level (except for direction 7), for the first five assessment dates (up to 59 days after inoculation) on the most homogeneous plot, P3 (Fig. 6). The model based on eight assessment dates underestimated disease levels (with values <0.05). During the initial period, estimates of the velocity of disease spread (c) were generally close to the mean for the whole assessment period, with steeper disease gradients (b), indicating dispersion over shorter distances, associated with lower rates of progression over time. For P2, the model correctly predicted disease variations (except for directions 3 and 6) over the same time period. The disease velocity was slower than that for the epidemic as a whole. After day 59 (2 July), the model underestimated the probability of a leaf becoming infected for both plots, resulting in poor prediction of disease spread at vine level ($P < 0.05$). For plot P1, disease levels were low, probably due to the low vigor of the vines, resulting in poor prediction of disease spread at the vine level regardless of the period considered.

Spread of the epidemic from multiple natural foci. *Description of the disease: disease development is similar to that on a small, artificially inoculated plot.* The temporal progression of the disease was similar to that observed on P2, with 15% of leaves and 88% of vines showing signs of disease by 15 June (≈ 43 days after the observation of the primary foci) (Fig. 7C). Overall, disease development on quadrats of 45 vines surrounding primary foci was similar to the entire plot. It took a maximum delay of 12 days to reach similar levels of disease between quadrats of the same size (45 vines) separated by ≈ 15 to 16 m and including the four primary foci (V4-F1, V19-F2, and V35-F3F4) or not including those foci (V50) (Figs. 7A and B and 8). The overall aggregation pattern was very similar to that in plots P3 and P1 (Fig. 7C).

Characterization of primary foci: disease gradient and velocity are focus dependent. The hypotheses accepted in the likelihood ratio tests (Table 2, models M1 and M2) were consistent with a constant rate of disease spread over time, with parameters b (gradient slope), c (velocity of spread), and K (inverse of initial inoculum) dependent on the focus, and identical anisotropy for each focus (a constant), consistent with prevailing wind direction or row structure, having the strongest effects on disease spread (Table 4). The disease spread faster along the between-rows direction, as indicated by the a value. Focus F1 (R2-V4) was

unusual in that foliar disease incidence did not increase on the source vine. Therefore, estimates of parameter values were incorrect with, for example, negative disease velocity. Disease spread from F2 (R2-V19) was much slower than that from F3 and F4, with a lower velocity of spread (by a factor of 30) and a steeper slope of disease gradient. F3 and F4 displayed very similar characteristics with a similar velocity of spread. In this plot (P4) with multiple natural foci, the velocity of spread of focus F2 was lower than that on inoculated plot P1 to P3 (one-half that of P1 and one-eighth that of P2) and those of foci F3 and F4 were much higher than that on the inoculated plots (13 times higher than for P1 and 4 times higher than for P2).

Model validation: the early part of the epidemic determining the risk of damage to grape is well predicted by the logistic model. The change in the probability of a leaf becoming infected over time was well described by the spatiotemporal multiple-focus model, at least until early July (≈ 3 weeks after flowering). Thereafter, the model overestimated the probability of a leaf becoming infected (Fig. 9). The probability of a leaf becoming infected during the 13 days after flowering (between flowering on 2 June and 15 June) increased from 2.5 to 13%, values similar to those predicted by the temporal logistic model for the artificially inoculated plot with vigorous growth, P2 (3.5 to 16.1% between flowering on 10 June and 24 June).

TABLE 3. Parameter estimates (equation 2) and hypothesis test based on the calculation of the probability of leaves becoming infected

Effect, level ^w	Likelihood (L)	Estimated parameters ^x			Days ^y	Likelihood test ^z			df	χ^2
		K	b	c		2 Δ l				
S										
m1										
Experiment	L1	5,201.947	6.08	0.44	0.25	4.0	L ₁ -L _G	473.48	69	97.96
P										
m2										
P1	L2 P1	1,337.259	4.84	0.50	0.15	6.5	L ₂ -L _G	164.72	63	82.52
P2	L2 P2	2,038.106	6.76	0.27	0.45	2.2				
P3	L2 P3	1,672.206	7.32	0.72	0.19	5.4				
	L2	5,047.57								
D										
m3										
d1 (N)	L3 d1	611.371	6.44	0.90	0.13	7.7	L ₃ -L _G	413.49	48	65.1
d2 (NE)	L3 d2	650.440	6.49	0.46	0.26	3.9				
d3 (E)	L3 d3	652.837	5.49	0.43	0.23	4.3				
d4 (SE)	L3 d4	621.913	6.19	0.58	0.20	5.0				
d5 (S)	L3 d5	653.155	5.83	0.81	0.13	7.5				
d6 (SW)	L3 d6	661.651	6.17	0.31	0.36	2.8				
d7 (W)	L3 d7	663.629	6.13	0.30	0.35	2.8				
d8 (NW)	L3 d8	656.960	6.39	0.43	0.27	3.7				
	L3	5,171.95								
D/P										
mG										
P1 d1	L _G P1 d1	110.093	4.58	1.99	0.04	26.2	L _G P1-L ₂ P1	64.6	21	32.67
P1 d2	L _G P1 d2	159.062	4.37	0.41	0.17	6.0				
P1 d3	L _G P1 d3	184.659	5.36	0.69	0.13	7.7				
P1 d4	L _G P1 d4	182.678	6.74	0.64	0.19	5.4				
P1 d5	L _G P1 d5	192.278	4.59	0.61	0.13	7.9				
P1 d6	L _G P1 d6	173.913	5.47	0.46	0.19	5.2				
P1 d7	L _G P1 d7	159.700	4.86	0.59	0.13	7.6				
P1 d8	L _G P1 d8	142.584	4.49	0.49	0.14	7.2				
	L _G P1	1,304.967								
P2 d1	L _G P2 d1	247.077	7.50	0.78	0.17	5.8	L _G P2-L ₂ P2	63.60	21	32.67
P2 d2	L _G P2 d2	233.921	6.76	0.38	0.33	3.0				
P2 d3	L _G P2 d3	230.508	6.19	0.21	0.57	1.7				
P2 d4	L _G P2 d4	236.540	5.99	0.39	0.30	3.3				
P2 d5	L _G P2 d5	261.245	6.12	0.81	0.15	6.8				
P2 d6	L _G P2 d6	260.539	7.48	0.13	0.99	1.0				
P2 d7	L _G P2 d7	266.553	7.49	0.12	1.10	0.9				
P2 d8	L _G P2 d8	269.910	7.76	0.39	0.37	2.7				
	L _G P2	2,006.293								
P3 d1	L _G P3 d1	217.247	7.91	0.86	0.17	6.0	L _G P3-L ₂ P3	36.50	21	32.67
P3 d2	L _G P3 d2	237.672	8.35	0.62	0.24	4.1				
P3 d3	L _G P3 d3	217.185	6.97	0.46	0.27	3.6				
P3 d4	L _G P3 d4	188.939	7.55	0.81	0.17	5.7				
P3 d5	L _G P3 d5	188.120	7.09	1.32	0.10	10.1				
P3 d6	L _G P3 d6	195.974	7.02	0.84	0.15	6.5				
P3 d7	L _G P3 d7	204.700	6.84	0.78	0.15	6.5				
P3 d8	L _G P3 d8	204.111	7.56	0.81	0.17	5.9				
	L _G P3	1,653.949
	L _G	4,965.21

^w Effect studied, model designation, experiment, and level tested S = experiment, P = plot, D = direction, and D/P = direction per plot.

^x K = constant related to the quantity of primary inoculum, b = the rate of decrease of the disease severity with the distance d to the source, and c = disease velocity.

^y Days to progress of 1 m.

^z Restricted (null) hypothesis is a subset of the unrestricted (general) hypothesis, direction, experiment, or plot effect. When the null hypothesis is a subset of the alternative hypothesis, 2 Δ l is distributed according to a χ^2 distribution with p degrees of freedom under the null hypothesis, where p is the difference in the number of free parameters between the general and restricted model. The assumption is then rejected if the 2 Δ L value is significantly larger than a χ^2 percentile with p degrees of freedom (p = df G-df submodel); χ^2 indicates χ^2 threshold.

The empirical variograms along the rows at each assessment date (Fig. 10) provided information about the spatial distribution of new infections on leaves measuring the similarity between plant disease levels depending on their distance. Their slope indicates that the difference in the number of leaves becoming diseased increased with the distance between vines, demonstrating the existence of spatial heterogeneity. This structure was maintained until the end of the epidemic. Just before flowering (day 146), the variogram was within the confidence interval, indicating that the model correctly predicted intraplot variation. However, from day 153 (2 June) to day 166 (15 June), the model underestimated spatial variation. In the observed epidemic, no strong distance effect was observed after day 166 (variations of disease with distance stabilized).

The model described well the distribution of numbers of newly infected leaves along the row (spatial extension of the disease) (Fig. 11). Foci F2 and F3-F4 dominated the model and the data, although the model predicted less variation than was actually observed around the foci. At the end of the epidemic, the model did not take into account a possible saturation effect, with a lack of healthy leaves available for infection.

DISCUSSION

In this study, the spatiotemporal progression and spread of powdery mildew epidemics on vines was described and analyzed by fitting simple logistic models to disease data obtained in the field. We considered changes in the probability of a leaf becoming infected over time without using more complicated models, including specific parameters for host growth or host susceptibility (26,52). Models characterizing the progression and spread of the

epidemic were fitted to count data and subjected to statistical analysis. With these models, we were able to predict changes in disease over time and of its extension within the plot. However, crop heterogeneity prevented prediction of variability of the disease at the vine scale. Our approach, by taking into account the variability of parameters and the ability of the models to predict disease at different scales, improved our knowledge of environmental factors directly or indirectly (through the crop structure) affecting the probability of the host becoming infected.

The logistic model was able to predict the overall spread of the disease over time throughout the entire plot, at least for the main part of the epidemic. Better predictions were obtained for the multiple foci model, which takes into account the lack of independence of primary foci. Just after flowering, when the disease is transmitted from leaves to grape clusters, the probability of new infection increases from 2.5 to 13% in 15 days. This increase in the probability of infection at this time point in vine growth may be a good indicator of epidemics associated with a high risk of damage.

However, because the logistic model does not explicitly take secondary spread into account, its use should be limited to the first part of the epidemic, before the disease spreads to all vines. The model could be used on small plots to compare epidemics in different environments (vigor, with or without secondary shoots, various isolates, inoculum pressure, date of inoculation, cultivars, and so on). Disease prediction at vine level, based on the multiple-foci spatiotemporal model, should be restricted to the first part of the epidemic just before flowering (end of May). The spatiotemporal model is able to predict the average disease extension (Fig. 11) on the plot. Spatial prediction could also be substantially improved by considering the multiplication of sec-

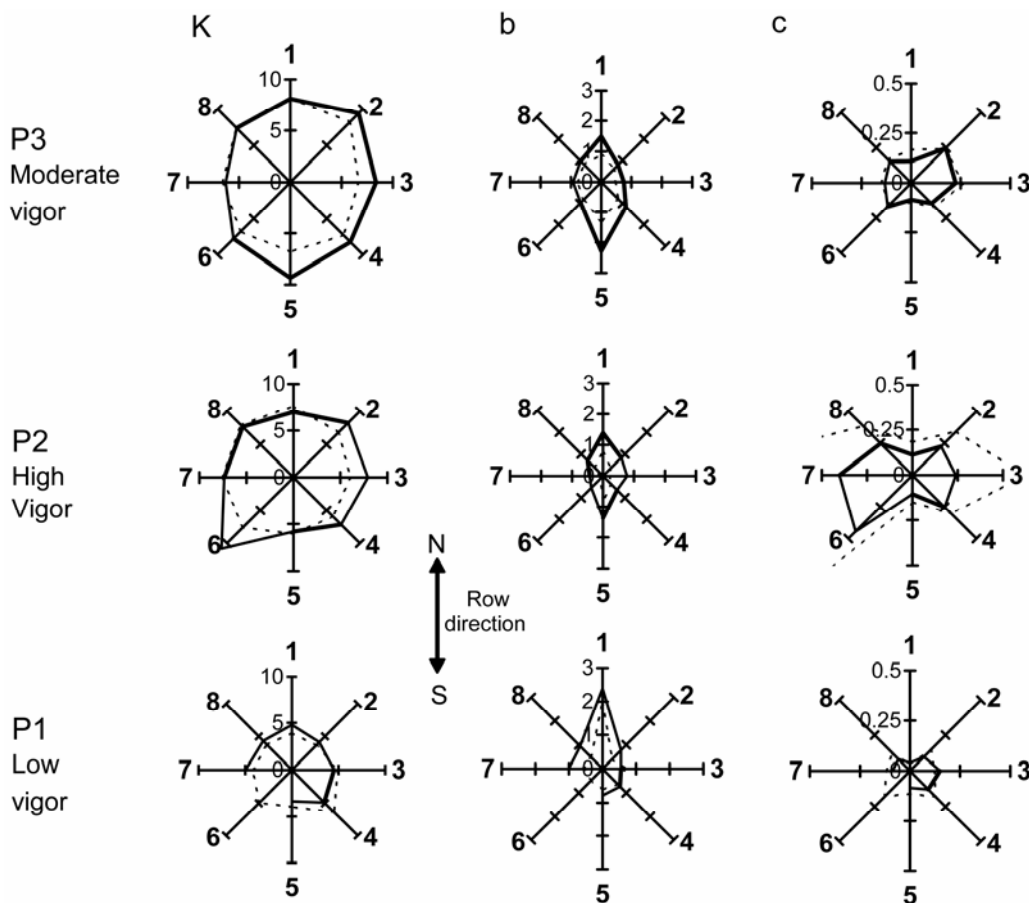


Fig. 6. Comparison of the parameter estimates K , b , and c (equation 2) for grape powdery mildew for the eight cardinal directions (1 = north to 8 = northwest) and three plots (P1, P2, and P3), with estimates based on the first five assessments dates (bold line, $P > 0.05$; fine line, $P < 0.05$), or on the eight assessments dates (dashed lines).

ondary colonies and foci (40) and by using predictions conditionally on previously observed data. This approach might also correct possible uncertainties concerning the nonidentification of unidentified primary foci due to late ascospore release and disease censoring. Prediction methods based on a single snapshot (30), such as the highest phenological stage reached after flowering, could probably not be used in this situation because such methods require the conservation of basic spatial patterns over time and can deal with only moderate spatial heterogeneity.

Artificially inoculated plots, on which primary infection was easy to monitor over space and time, gave a precise characterization of disease spread. An analysis of these plots showed potentially high levels of variation in the spread of the disease over time and space in a given year and area. Comparisons of parameter value at different scales (site, plot, and direction) and by analysis of the qualitative relationships between disease and vigor maps showed that the spatial spread of powdery mildew was strongly related to the vigor of the vine and, to a lesser extent, to the direction of the prevailing wind only visible on the most homogenous plot. Both these factors decreased the slope of disease gradient parameter (spread over a longer distance in vigorous crops or in the direction of the prevailing wind). Row structure had the opposite effect, with the velocity of spread of the epidemic being slowed down along the row. The extreme values ($0.04\text{--}1.1\text{ m day}^{-1}$) indicate that there may be a difference of up to 25 days between the onset of disease in favorable (high

vigor, adjacent rows) and unfavorable (low vigor, within row) areas. This delay may considerably change the level of damage (6). The average value for the site, 0.25 m day^{-1} , is within the range of observed values in airborne pathogen: velocities of 0.09 to 0.9 m day^{-1} have been reported for wheat (49) or oat crown rust (3).

Our comparison of parameters provides the first demonstration of the vigor effect on powdery mildew disease spread. Although not surprising for a biotrophic fungus highly dependent on the physiological state of its host (15,28,39), this effect on disease spread in the field was quantified for the first time here. The difference in disease between the two plots with high (P2) and moderate (P3) mean levels of vigor was detected in the epidemic as early as the second assessment date (10 June, beginning of flowering). Vigorous vines may be more susceptible due to a higher propensity of their tissues to become infected or to the production of larger amounts of inoculum on vigorous vines due to the larger number of diseased secondary leaves. Recent studies (47,48) have shown that the greater development of secondary leaves on vigorous vines is a key factor in the higher disease severity on leaves and grape berries. However, only controlled studies of infection process (e.g., after *in vitro* inoculation) for various host architecture would make it possible to determine which of the two hypotheses (higher source of inoculum or higher susceptibility of the source) is correct.

In the naturally infected plot with multiple foci, similar disease characteristics were observed: potential heterogeneity between

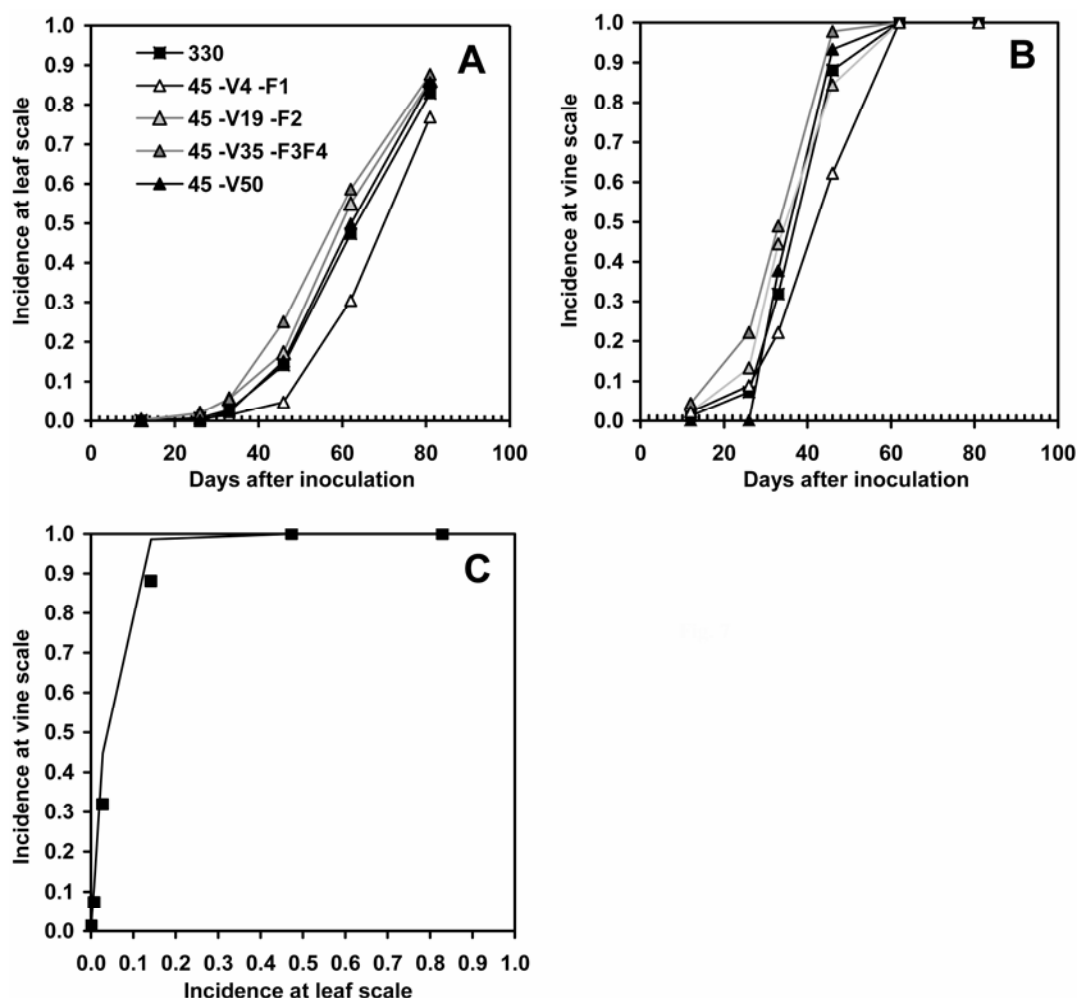


Fig. 7. Progression of powdery mildew over time during natural epidemics with **A**, incidence at leaf scale and **B**, incidence at vine scale for all 330 vines or for quadrats of similar sizes (45 vines) ≈ 15 to 16 m apart, including (V4-F1, V19-F2, and V35-F3F4) or not including (V50) the four primary foci. **C**, Observed relationship between two levels of spatial hierarchy: incidence at leaf scale (proportion of diseased leaves per vine with at least one colony) and incidence at vine scale (proportion of vines with at least one diseased leaf) for the whole plot, and simulated relationship according to a random (binomial) distribution of infected leaves (line).

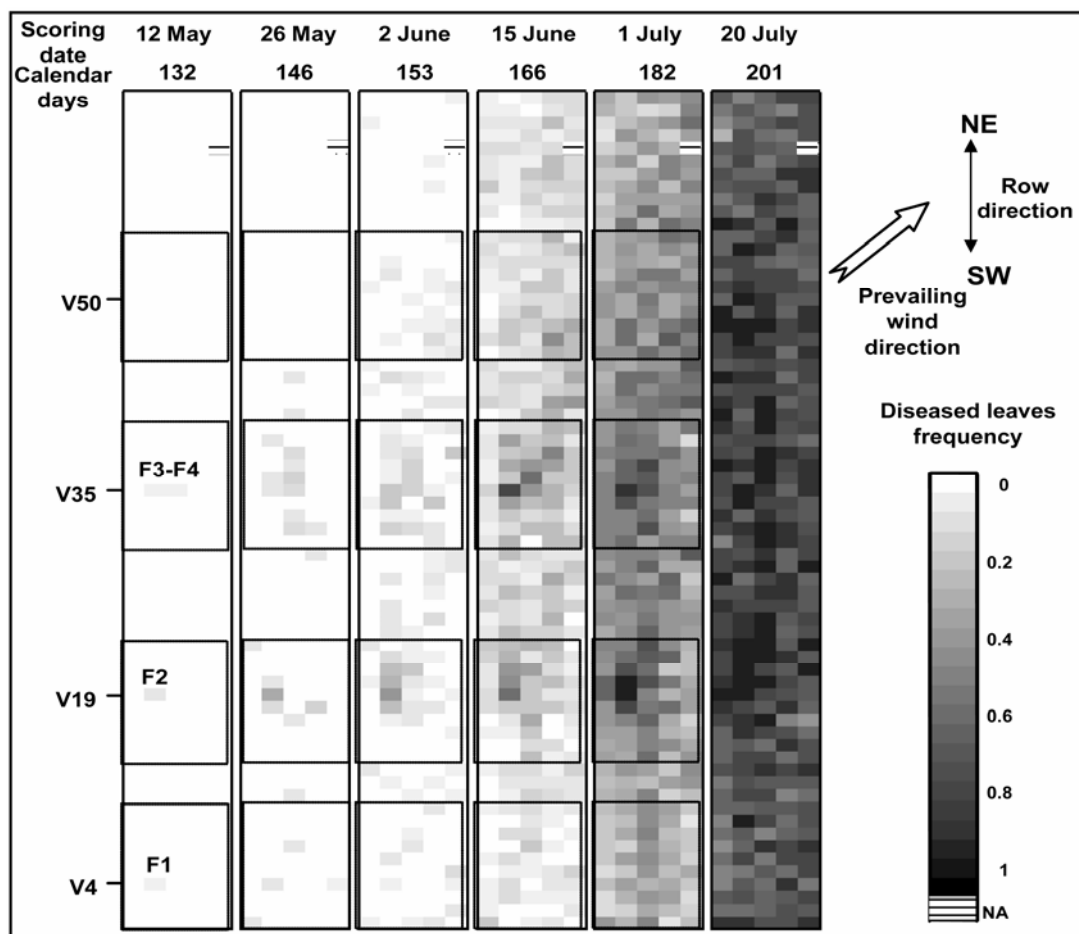


Fig. 8. Progression of powdery mildew over time and space on the 330-vine plot during natural epidemics. Grayscale density indicates the frequency of diseased leaves. Primary foci (F1–F4) are located at vine coordinates V4 (F1), V19 (F2), and V35 (F3 and F4). Quadrats of 45 vines are surrounded by a line.

TABLE 4. Characteristics of the primary foci for the site of Couhins on natural inoculations

Focus no.	Estimated parameters ^y			
	K	b	c	a
F1 ^z	2.77	1.78	-1.66	5.14
F2	2.83	1.64	0.06	5.14
F3	3.47	0.09	1.77	5.14
F4	3.04	0.07	1.8	5.14

^y K = constant related to the quantity of primary inoculum, b = the rate of decrease of the disease severity with the distance d to the source, c = disease velocity, and a = anisotropy of the horizontal disease spread.

^z Foliar disease incidence did not increase on the source vine, leading to incorrect parameters estimations.

foci and the slowing down of disease spread along the row, with dispersion supported by the prevailing wind. The velocity and extent of disease spread were also found to be of an order of magnitude similar to those for spread from an isolated focus. The spatial model predicted more limited spatial spread for F2 than for F3 and F4, with the probability of infection decreasing rapidly with distance from the center of the focus (almost zero at 6 m from the center of the focus). Several hypotheses may account for these variations and may be related to the models themselves, or to the biology of the system. These hypotheses include (i) an effect of the genetic origin of the isolates initiating the primary foci (biotype A for F2 and biotype B for F3 and F4): a lower level of aggressiveness or percentage germination of biotype A might have limited spread from F2 (37); (ii) the orientation of the plot with respect to the prevailing wind direction may have favored more intensive infection of the northeastern part of the plot; and

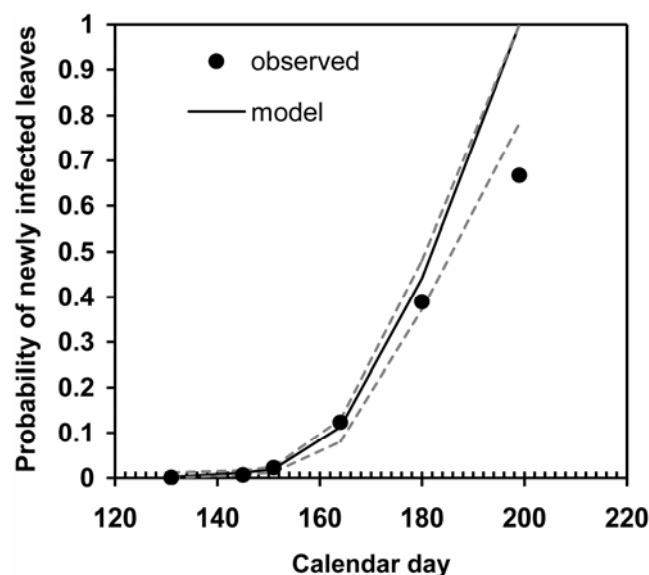


Fig. 9. Progression of powdery mildew over time, showing the observed (marks) and estimated (bold line) numbers of leaves that have recently become diseased, based on the spatial model with multiple foci (equation 2). Confidence intervals obtained after parametric bootstrap indicated in dashed lines.

(iii) a progressive gradient of vigor or physiological state of the vines, not visually identified, may have led to variation.

The velocity of disease spread was highly variable and depended on the focus considered. However, the rate of horizontal

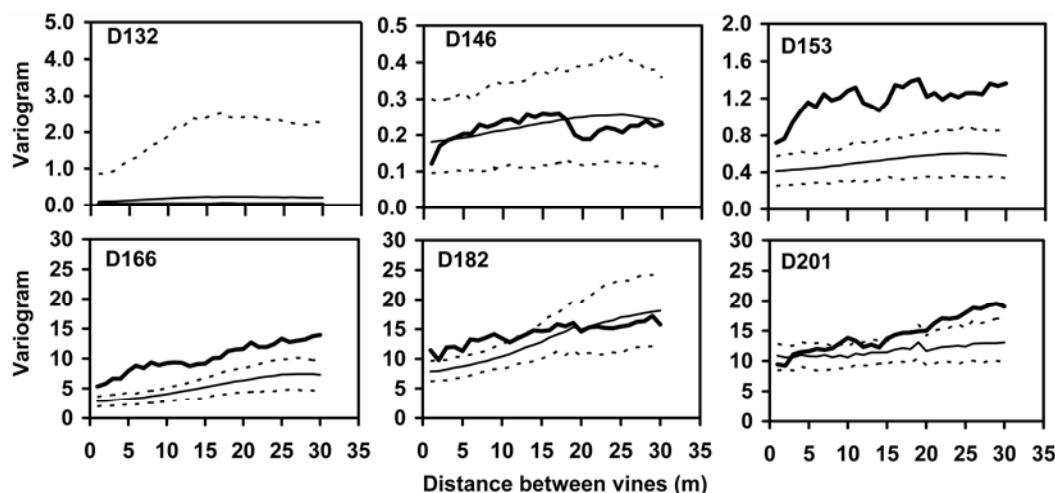


Fig. 10. Variograms for leaves newly infected with grape powdery mildew for six assessments dates (calendar day D132–D201), based on observed data (bold line) or on the spatial model with multiple foci (fine line) and their confidence intervals obtained after parametric bootstrap (dashed lines).

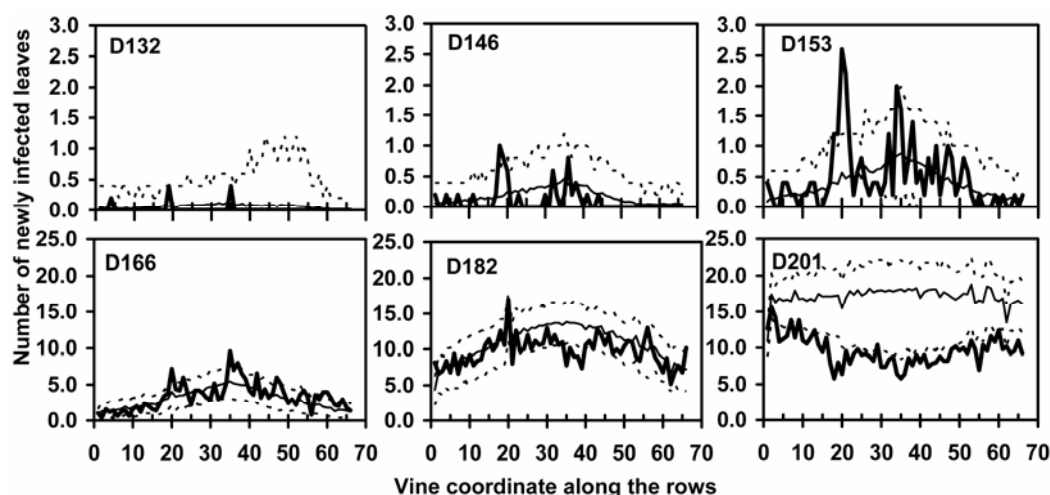


Fig. 11. Extension along the row of leaf infection with grape powdery mildew on the six assessments dates (calendar days D132–D201): observed data (bold line), spatial model with multiple foci (fine line), and their confidence intervals obtained after parametric bootstrap (dashed lines).

spread was similar for the various foci of the naturally infected plot P4 (0.06 to 1.8 m day⁻¹) and for the foci of the inoculated plots P1, P2, and P3 (0.04 to 1.1 m day⁻¹). Furthermore, the similar relationship between disease incidence at the leaf scale and at the vine scale for plots of 49 vines or 330 vines in two different years indicates strong characteristics for the dispersion process: a dispersion of conidia with similar proportion of short and long distance and not tightly dependant on climate (27,33). This finding is consistent with mathematical models showing that there is an optimal proportion of spores dispersed at short and long distances for an efficient disease spread (54). This optimal proportion of spores dispersed at short and long distances is affected by row structure (5,16,54). Factors affecting the amount of spores produced, such as vigor and pathogen aggressiveness, may also affect the numbers of spores traveling over longer distances and, therefore, the rate of invasion.

For disease control as part of an integrated pest management system or in precision agriculture, in which treatments are restricted to a minimum, it would be important to be able to predict disease variation at flowering, and the area or plots with a potential high risk of disease and variability in disease at this period. Indeed, the amount of disease on leaves at flowering is a good predictor of damage on grape. Our results demonstrate the major effects of disease variability due to crop effects (vigor and row structure) and pathogen variability during this period. The

temporal logistic model correctly predicted disease variation at flowering and, if the spatiotemporal model failed to predict disease variation at the vine scale, it is able to predict average disease extension on the plot. Prediction of disease extension in areas with the potential highest risk of disease extension may be useful for precision agriculture. The power of prediction would depend on the amount of data available and on identification of the primary foci.

ACKNOWLEDGMENTS

We thank A. Franc and C. Lannou for their useful comments and correction of the manuscript.

LITERATURE CITED

1. Aubertot, J. M., Barbier, J. M., Carpentier, A., Gril, J. J., Guichard, L., Lucas, P., Savary, S., Savini, I., and Voltz, M. 2005. Pesticides, agriculture et environnement. Réduire l'utilisation des pesticides et limiter leurs impacts environnementaux. Rapport d'expertise collective. INRA, Paris. CEMAGREF, Antony Ed. Quae.
2. Baggiolini, A. 1952. Les stades repérés dans le développement annuel de la vigne et leur utilisation pratique. Rev. Romande Agric. Vitic. Arboric. 8:4-6.
3. Berger, R. D., and Luke, H. H. 1979. Spatial and temporal spread of oat crown rust. Phytopathology 69:1199-1201.

4. Blaise, P., and Gessler, C. 1992. An extended progeny/parent ratio model: II. Application to experimental data. *J. Phytopathol.* 134:53-62.
5. Burie, J. B., Calonnec, A., and Langlais, M. 2007. Modeling of the invasion of a fungal disease over a vineyard. *Mathematical modeling of biological systems. Series: Modeling and Simulation in Science, Engineering and Technology II*:11-21. Birkhauser Boston Publishing, Bale (CHE).
6. Calonnec, A., Cartolaro, P., Deliere, L., and Chadoeuf, J. 2006. Powdery mildew on grapevine: The date of primary contamination affects disease development on leaves and damage on grape. *IOBC/WPRS Bull.* 29:67-73.
7. Calonnec, A., Cartolaro, P., Poupot, C., Dubourdieu, D., and Darriet, P. 2004. Effects of *Uncinula necator* on the yield and quality of grapes (*Vitis vinifera*) and wine. *Plant Pathol.* 53:434-445.
8. Campbell, C. L., and Madden, L. V., eds. 1990. Introduction to plant disease epidemiology. In: *Introduction to Plant Disease Epidemiology*. John Wiley & Sons, New York.
9. Cartolaro, P., and Steva, H. 1990. Control of powdery mildew in the laboratory. *Phytoma* 419:37-40.
10. Cox, D. R., and Hinkley, D. V., eds. 1974. *Theoretical Statistics*. Chapman & Hall, London.
11. Darriet, P., Pons, M., Henry, R., Dumont, O., Findeling, V., Cartolaro, P., Calonnec, A., and Dubourdieu, D. 2002. Impact odorants contributing to the fungus type aroma from grape berries contaminated by powdery mildew (*Uncinula necator*): Incidence of enzymatic activities of the yeast *Saccharomyces cerevisiae*. *J. Agric. Food Chem.* 50:3277-3282.
12. Delye, C., and Corio-Costet, M. F. 1998. Origin of primary infections of grape by *Uncinula necator*: RAPD analysis discriminates two biotypes. *Mycol. Res.* 102:283-288.
13. Delye, C., Laigret, F., and Corio-Costet, M. F. 1997. RAPD analysis provides insight into the biology and epidemiology of *Uncinula necator*. *Phytopathology* 87:670-677.
14. Efron, B., and Tibshirani, R., eds. 1993. *An Introduction to the Bootstrap*. Chapman & Hall, London.
15. Evans, K., Crisp, P., and Scott, E. S. 2006. Applying spatial information in a whole-of-block experiment to evaluate spray programs for powdery mildew in organic viticulture. *Proc. 5th Int. Workshop Grapevine Downy and Powdery Mildew*. I. Pertot, C. Gessler, D. Gadoury, W. Gubler, H.-H. Kassemeyer, and P. Magarey, eds. SafeCrop, Italy.
16. Ferrandino, F. 1993. Dispersive epidemic waves: I. Focus expansion within a linear planting. *Phytopathology* 83:795-802.
17. Ficke, A., Gadoury, D. M., and Seem, R. C. 2002. Ontogenic resistance and plant disease management: A case study of grape powdery mildew. *Phytopathology* 92:671-675.
18. Ficke, A., Gadoury, D. M., Seem, R. C., and Dry, I. B. 2003. Effects of ontogenic resistance upon establishment and growth of *Uncinula necator* on grape berries. *Phytopathology* 93:556-563.
19. Gadoury, D. M., Seem, R. C., Ficke, A., and Wilcox, W. F. 2003. Ontogenic resistance to powdery mildew in grape berries. *Phytopathology* 93:547-555.
20. Gessler, C., and Blaise, P. 1992. An extended progeny/parent ratio model: II. Application to experimental data. *J. Phytopathol.* 134:53-62.
21. Gibson, G. J. 1997. Investigating mechanisms of spatio-temporal epidemic spread using stochastic models. *Phytopathology* 87:139-146.
22. Gibson, G. J., and Austin, E. J. 1996. Fitting and testing spatio-temporal stochastic models with application in plant epidemiology. *Plant Pathol.* 45:172-184.
23. Gosme, M. 2008. How to analyze spatial structure and model spatio-temporal development of epiphytes? *Can. J. Plant Pathol. Rev. Can. Phytopathol.* 30:4-23.
24. Gottwald, T. R., Cambra, M., Moreno, P., Camarasa, E., and Piquer, J. 1996. Spatial and temporal analyses of citrus tristeza virus in eastern Spain. *Phytopathology* 86:45-55.
25. Gottwald, T. R., Timmer, L. W., and McGuire, R. G. 1989. Analysis of disease progress of citrus canker in nurseries in Argentina. *Phytopathology* 79:1276-1283.
26. Hau, B. 1990. Analytic models of plant disease in a changing environment. *Annu. Rev. Phytopathol.* 28:221-245.
27. Hughes, G., McRoberts, N., Madden, L. V., and Gottwald, T. R. 1997. Relationships between disease incidence at two levels in a spatial hierarchy. *Phytopathology* 87:542-550.
28. Jarvis, W. R., Gubler, W. D., and Grove, G. G. 2002. Epidemiology of powdery mildews in agricultural pathosystems. In: *The Powdery Mildews. A Comprehensive Treatise*. R. Bélanger, R. Bushnell, A. Dik, and T. Carver, eds. The American Phytopathological Society, St. Paul, MN.
29. Jeger, M. J. 1983. Analysing epidemics in time and space. *Plant Pathol.* 32:5-11.
30. Keeling, M. J., Brooks, S. P., and Gilligan, C. 2004. Using conservation of pattern to estimate spatial parameters from a single snapshot. *Proc. Natl. Acad. Sci. USA* 101:9155-9160.
31. Madden, L. V. 2006. Botanical epidemiology: Some key advances and its continuing role in disease management. *Eur. J. Plant Pathol.* 115:3-23.
32. Madden, L. V., and Hughes, G. 1999. Sampling for plant disease incidence. *Phytopathology* 89:1088-1103.
33. McRoberts, N., Hughes, G., and Madden, L. V. 2003. The theoretical basis and practical application of relationships between different disease intensity measurements in plants. *Ann. Appl. Biol.* 142:191-211.
34. Nelson, S. C. 1995. Spatio-temporal distance class analysis of plant-disease epidemics. *Phytopathology* 85:37-43.
35. Park, A. W., Gubbins, S., and Gilligan, C. 2001. Invasion and persistence of plant parasites in a spatially structured host population. *Oikos* 94:162-174.
36. Pearson, R. C., and Gadoury, D. M. 1992. Powdery mildew of grape. In *Plant Diseases of International Importance. Volume III. Diseases of fruit Crops*. J. Kumar, H. S. Chaube, U. S. Singh and A. N. Mukhopadhyay, eds. Prentice Hall, Englewood Cliffs, NJ.
37. Peros, J. P., Nguyen, T. H., Troulet, C., Michel-Romiti, C., and Notteghem, J. L. 2006. Assessment of powdery mildew resistance of grape and *Erysiphe necator* pathogenicity using a laboratory assay. *Vitis* 45:29-36.
38. Peyrard, N., Calonnec, A., Bonnot, F., and Chadoeuf, J. 2005. Explorer un jeu de données sur grille par tests de permutation. *Rev. Stat. Appl. LIII*:59-78.
39. Rapiilly, F. 1991. *L'Epidémiologie en Pathologie Végétale: Mycoses Aériennes*. Institut National de la Recherche Agronomique, Paris.
40. Ripley, B. D. 1988. *Statistical Inference for Spatial Processes*. Cambridge University Press.
41. Rumbolz, J. 1999. Untersuchungen zur Konidienkeimung und Mycelentwicklung des Echten Mehltaus der Weinrebe (*Uncinula necator* (Schw.) Burr.) und deren Einfluss auf die Epidemiologie. Thesis, University of Konstanz.
42. Sache, I., and Zadoks, J. C. 1996. Spread of faba bean rust over a discontinuous field. *Eur. J. Plant Pathol.* 102:51-60.
43. Sall, M. 1980. Epidemiology of grape powdery mildew: A model. *Phytopathology* 70:338-342.
44. Soubeyrand, S., Sache, I., Lannou, C., and Chadoeuf, J. 2007. A frailty model to assess plant disease spread from individual count data. *J. Data Sci.* 5:67-83.
45. Sweetmore, A., Simons, S. A., and Kenward, M. 1994. Comparison of disease progress curves for yam anthracnose (*Colletotrichum gloeosporioides*). *Plant Pathol.* 43:206-215.
46. Thebaud, G., Peyrard, N., Dallot, S., Calonnec, A., and Labonne, G. 2005. Investigating disease spread between two assessment dates with permutation tests on a lattice. *Phytopathology* 95:1453-1461.
47. Valdes, H. 2007. Relations entre états de croissance de la vigne et maladies cryptogamiques sous différentes modalités d'entretien du sol en région méditerranéenne. Thesis, Agronomie, Science du sol, Univ. Ecole de Montpellier supAgro, Montpellier, France.
48. Valdes, H., Celette, F., Fermaud, M., Cartolaro, P., Clerjeau, M., and Gary, C. 2005. How to evaluate the influence of vegetative vigour in grape vine susceptibility to cryptogamic diseases. *Proc. XIV Int. GESCO Viticult. Congr.* H. R. Schultz ed. Geisenheim.
49. Van den Bosch, F., Zadoks, J. C., and Metz, J. A. J. 1988. Focus expansion in plant disease. III. Two experimental examples. *Phytopathology* 78:919-925.
50. Van der plank, J. E. 1963. *Plant Diseases: Epidemics and Control*. Academic Press, New York and London.
51. Venzon, D. J., and Moolgavka, S. H. 1988. A method for computing profile likelihood based confidence intervals. *Appl. Stat.* 37:87-94.
52. Waggoner, P. E. 1986. Progress curves of foliar diseases: Their interpretation and use. In: *Plant Disease Epidemiology*. K. J. Leonard and W. E. Fry, eds. MacMillan, New York.
53. Waggoner, P. E., and Rich, S. 1981. Lesion distribution, multiple infection, and the logistic increase of plant disease. *Proc. Natl. Acad. Sci. USA* 78:3292-3295.
54. Zawolek, M. W., and Zadoks, J. C. 1992. Studies in focus development: An optimum for the dual dispersal of plant pathogens. *Phytopathology* 82:1288-1297.